"An oscillator-based smooth real-time estimate of gait phase for wearable robotics"

Yan, Tingfang ; Parri, Andrea ; Ruiz Garate, Virginia ; Cempini, Marco ; Ronsse, Renaud ; Vitiello, Nicola

ABSTRACT

This paper presents a novel methodology for estimating the gait phase of human walking through a simple sensory apparatus. Three subsystems are combined: a primary phase estimator based on adaptive oscillators, a desired gait event detector and a phase error compensator. The estimated gait phase is expected to linearly increase from 0 to 2π rad in one stride and remain continuous also when transiting to the next stride.We designed two experimental scenarios to validate this gait phase estimator, namely treadmill walking at different speeds and free walking. In the case of treadmill walking, the maximum phase error at the desired gait events was found to be 0.155 rad, and the maximum phase difference between the end of the previous stride and beginning of the current stride was 0.020 rad. In the free walking trials, phase error at the desired gait event was never larger than 0.278 rad. Our algorithm outperformed against two other benchmarked methods. The good performance of our gait phase estimator could provide consistent and finely tuned assistance for an exoskeleton designed to augment the mobility of patients.

CITE THIS VERSION

Yan, Tingfang ; Parri, Andrea ; Ruiz Garate, Virginia ; Cempini, Marco ; Ronsse, Renaud ; et. al. *An oscillator-based smooth real-time estimate of gait phase for wearable robotics.* In: *Autonomous Robots*, Vol. 41, no. 3, p. 759–774 (2017) http://hdl.handle.net/2078.1/174471 -- DOI : 10.1007/s10514-016-9566-0

An oscillator-based smooth real-time estimate of gait phase for wearable robotics

Tingfang Yan · Andrea Parri · Virginia Ruiz Garate · Marco Cempini · Renaud Ronsse · Nicola Vitiello

Abstract This paper presents a novel methodology for estimating the gait phase of human walking through a simple sensory apparatus. Three subsystems are combined: a primary phase estimator based on adaptive oscillators, a desired gait event detector and a phase error compensator. The estimated gait phase is expected to linearly increase from 0 to 2π rad in one stride and remain continuous also when transiting to the next stride. We designed two experimental scenarios to validate this gait phase estimator, namely treadmill walking at different speeds and free walking. In the case of treadmill walking, the maximum phase error at the desired gait events was found to be 0.155 rad, and the maximum phase difference between the end of the previous stride and beginning of the current stride was 0.020 rad. In the free walking trials, phase error at the desired gait event was never larger than 0.278 rad. Our algorithm outperformed against two other benchmarked methods. The good performance of our gait phase estimator could provide consistent and finely tuned assistance for an exoskeleton designed to augment the mobility of patients.

Keywords Real-time gait phase estimate, adaptive oscillators, phase error learning, wearable robotics.

1 Introduction

Autonomous mobility is essential for daily-life activities. However, the prevalence of lower-limb mobility impairments is observed among people at different ages, especially the elderly (Iezzoni et al. 2001). It is estimated that up to 35% of people over 70 encounter problems in walking. This percentage increases to almost 60% at 80-84 years of age (Verghese et al. 2006). Gait impairments are thus widespread among elderly people and can lead to both physical and cognitive barriers: slower walking, health-risk situations, such as stumbling, and thus limited social participation or depression. In an era where various innovative technologies have been developed for daily-life services, wearable robotics designed to assist people with gait impairments is attracting great attention, for example lower-limb exoskeletons/orthoses.

The assistive functions of a lower-limb exoskeleton rely on the capabilities to: (i) "decode" the user's intended movement; and (ii) detect the real-time phase of this intended movement (Pons 2008). In particular, the success of these interpretations is fundamental for the assistive device to consistently act with natural gait biomechanics, thus restoring more functional and energy-efficient locomotion. In this study, we focus on the development of the second capability, i.e. acquiring an accurate and continuous gait phase for the locomotion task. For the purpose of a friendly and comfortable human-robot interface, the phase estimator is expected to be independent from a complex sensory apparatus.

In the literature, different methods of estimating the gait phase for powered lower-limb exoskeletons can be tracked (Yan et al. 2015). A classic approach is designed to firstly identify the human gait as a series of time-discrete states and then implement the encoded assistive function phase by phase. The discrete states can be easily recognized with wearable sensors, such as the application on the exoskeleton "BLEEX" (Kazerooni et al. 2006) and the transfemoral prosthesis in (Ambrozic et al. 2014). This approach – despite being relatively easy to be implemented through finite-state classifiers – has some limitations. First of all, the identification of each state only relies on the data fed back by a wearable sensory apparatus. Thus it is prone to induce a delay. Furthermore, the discrete states limit the possibility to smoothly provide and finely tune assistance as a continuous function of the locomotion phase.

In order to overcome these limitations, an alternative strategy to detect the gait phase in real time is developed by exploiting the biomechanical information received from the muscle level. This method could anticipate the movement detection before the actual kinematic change: for instance, the utilization by HAL (Kawamoto et al. 2010) and Michigan ankle foot orthosis (Kao et al. 2010). Nevertheless, a trade-off is that the robot-user interface turns out to be more complex, mainly due to the

T. Yan is the corresponding author,
The BioRobotics Institute, Scuola Superiore Sant'Anna, viale Rinaldo Piaggio 34, 56025 Pontedera (PI), Italy.
Tel.: +39 3334900778, Fax: +39 050883101.
E-mail: t.yan@sssup.it;

A. Parri (an.parri@sssup.it); M. Cempini (m.cempini@sssup.it).
The BioRobotics Institute, Scuola Superiore Sant'Anna, viale Rinaldo Piaggio 34, 56025 Pontedera (PI), Italy.

V. Ruiz Garate (virginia.ruizgarate@uclouvain.be); R. Ronsse (renaud.ronsse@uclouvain.be).
Louvain Bionics and Institute of Mechanics, Materials, and Civil Engineering, Université catholique de Louvain, Place du Levant, 2 bte L5.04.02 B-1348 Louvain-la-Neuve, Belgium.

N. Vitiello (n.vitiello@sssup.it)
The BioRobotics Institute, Scuola Superiore Sant'Anna, viale Rinaldo Piaggio 34, 56025 Pontedera (PI), Italy.
Don Carlo Gnocchi Foundation, Florence, Via di Scandicci, 265, Florence, Italy.

The first two authors contributed equally to this work.

placement of electrodes and the need for subject-specific or even trial-specific calibrations.

Another approach for replacing the discrete states with no added complexity is to acquire a continuous phase estimation of the locomotion task. Usually, in order to report the locomotion kinematics and kinetics, researchers consider an ideal gait phase that linearly increases from 0% to 100% in one cycle (Winter 2009). In the state of the art, there are three popular methods explored to build a continuous gait phase estimator online. In the first method, the duration of the current gait cycle is estimated as the average of previous stride periods. Starting from 0%, the phase then continuously increases with a constant frequency until the end of the current stride. In (Lewis and Ferris 2011), this method was employed to estimate the gait phase during walking and realize a bang-bang control for the Michigan hip exoskeleton. The second method is proposed by Lenzi et al. to monolaterally assist the hip movement with the exoskeleton ALEX II (Lenzi et al. 2013). They introduced a pool of adaptive oscillators (AOs) to synchronize with the moving frequency of the hip joint (Buchli et al. 2008; Righetti et al. 2006, 2009). As a consequence, stride duration continued to update even within one stride cycle. The gait phase was computed as a ratio between the time elapsing from the current gait cycle and the expected duration. In the third method, the gait phase does not depend on the prediction of cycle duration but on monitoring of the global tibia angle (Holgate et al. 2009). For controlling an active ankle prosthesis, the authors found that the polar angle between the tibia angle and its scaled angular velocity had an invertible relationship with the gait phase and was not subject-dependent. Consequently, a fitted function was built between the polar angle and gait phase. In other words, knowing the tibia angle and its angular velocity allowed the gait phase to be easily estimated online.

Although all three methods can obtain a continuous phase variable within one stride, there are some restrictions to be discussed. Firstly, the accuracy of the first two methods is determined by the accuracy of the predicted duration of the current gait cycle. Stride duration is affected by variations in gait speed, despite continuing to update within one stride in the second method. Then, according to the definition of the first two methods, regardless of its value at the end of a gait cycle, the gait phase is reset to 0% once the next cycle starts. As a consequence, at the stride to stride transition, a discontinuity may occur to the gait phase. Since the latter is the reference for an exoskeleton delivering assistance, this abrupt phase jump leads to discontinuous estimation of the desired torque or position, such as step-like variation. Even though this could be compensated by adding a filter in the exoskeleton's controller, the trade-off is the introduction of a delay which should be avoided. On the contrary, in the third method, the gait phase is affected neither by duration estimation nor by transition discontinuity. Still, it fundamentally depends on the quality of the tibia angle and its angular velocity. This means that the third method requires the sensory system to provide a stable and smooth tibia angle signal with reliable signal processing. In addition, the sensory signals also need to have simple quasi-sinusoidal envelopes like tibia angles, limiting their extension to other sensors. On top of this, the third method does not encode the dynamics of walking into its gait phase estimation, which means it would be affected immediately after occurrence of the sensory system failure.

The objective of this study is to propose an alternative phase estimation strategy which could preserve accuracy and continuity without loading the sensory system. We firstly aim to obtain a continuous phase by tracking a rhythmic locomotion signal. In the literature, several works have contributed to this dynamics estimation by using oscillators which could emulate the role of a biological central pattern generator (Buchli et al. 2008; Iwasaki 2008; Righetti et al. 2006). The oscillator presented in (Righetti et al. 2009) is able to learn the frequency of any periodic signal with a pool of AOs. As a result, no other specific requirement is needed for the desired input signal other than being periodic. Therefore, we selected AOs as our primary tool to estimate the gait phase and guarantee continuity. Then, in order to ensure the accuracy of the estimated gait phase, a phase error learning mechanism is designed to dynamically lock the zero phase with the starting moment of a gait cycle.

In this paper, the theoretical formulations of this novel gait phase estimator are presented in the first part of Section 2. The second part of Section 2 describes the validation experiments carried out with an active pelvis orthosis while the results are reported in Section 3. It is worth noting that in the results section, our method was benchmarked with other two methods in the state of the art. Finally, Section 4 and 5 draw the discussion and conclusion respectively.

2 Materials and Methods

This section reports the design of the gait phase estimator and the validation experiments. Specifically, the architecture and formulations for estimating the gait phase are presented in Subsection 2.1. Subsection 2.2 provides the details of the validation experiments carried out with an active pelvis orthosis.

2.1 Architecture of the gait phase estimator

The gait phase estimator consists of three subsystems dealing with event detection, AOs-based gait phase estimation, and phase error learning, respectively (see the three red-dashed boxes in Fig. 1). The first subsystem – the event detector – identifies the initialization of a new gait cycle at time t_k, which is represented by the occurrence of a desired biomechanical event (for example, toe off). The objective of the second

subsystem is to obtain a continuous phase variable $\varphi_n(t)$ by tracking a periodic biomechanical signal $\theta(t)$ with a pool of AOs. In this block, a phase error $\tilde{P}_e(t_k)$ is computed at the instant of event detection t_k. Then, the computed error is learned by a state variable $\varphi_e(t)$ in the third subsystem and used to smoothly correct the extracted phase $\varphi_n(t)$. Thanks to the three blocks, the final output gait phase $\phi(t)$ is expected to be continuous, accurate and synchronized to the desired gait event.

Formulations of each subsystem are presented in Subsections 2.1.2, 2.1.3, and 2.1.4 respectively. Though the tool (i.e. AOs) used to acquire the primary gait phase is cited from the literature, it is convenient for the reader to have a brief concept about its working principle before investigating our phase estimator. Thus, a recap of its working principles is addressed in Subsection 2.1.1. Interested readers can find further details in (Buchli et al. 2008; Righetti et al. 2006, 2009; Ronsse et al. 2011, 2013).

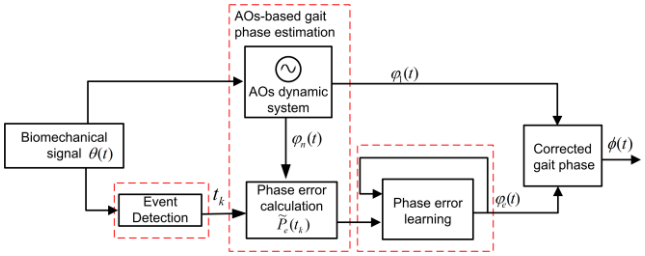

Fig. 1 Block diagram of the gait phase estimator. The three red-dashed boxes represent the three subsystems respectively: event detector, AOs-based gait phase estimator and phase error compensator. The first block contains the biomechanical signal. The corrected gait phase is output from the last block.

2.1.1 Adaptive Oscillators

The first use of AOs in the field of wearable robotics was proposed by some of the authors of this work in (Ronsse et al. 2011). The authors tried to obtain a fast estimation of the kinematics of cyclical tasks with no phase lag thus building assistive strategies for lower and upper orthoses. In particular, based on a set of state variables, AOs captured the fundamental features of a periodic signal, including phase, frequency, amplitude and offset. The input signal was then reconstructed in real time as a non-linear combination of the extracted variables. Differences between the input and reconstructed signals were fed back to the input to drive the dynamics of the state variables learning. A schematic diagram of the AO dynamic system is displayed in Fig. 2 and relevant formulations are given hereafter:

$$\dot{\varphi}_i(t) = \omega(t) \cdot i + \nu_\varphi \frac{F(t)}{\sum \alpha_i} \cos\big(\varphi_i(t)\big) \tag{1}$$

$$\dot{\omega}(t) = \nu_\omega \frac{F(t)}{\sum \alpha_i} \cos\big(\varphi_1(t)\big) \tag{2}$$

$$\dot{\alpha}_i(t) = \eta F(t) \sin\big(\varphi_i(t)\big) \tag{3}$$

$$\dot{\alpha}_0(t) = \eta F(t) \tag{4}$$

where ω is the fundamental frequency; φ_i, α_i are the phase and amplitude of the i-th oscillator respectively, capturing the contribution of the i-th harmonic; α_0 is the unique offset component. $F(t) = \theta(t) - \hat{\theta}(t)$ is the difference between the periodic input signal $\theta(t)$ and its estimate $\hat{\theta}(t)$, driving the evolution of each state variable along time t. The learning speeds of phase, frequency and amplitude are tuned by constant gains ν_φ, ν_ω and η. Reconstruction of the input signal is computed as a sum of the *N* harmonics:

$$\hat{\theta}(t) = \sum_{i=1}^{N} \alpha_i(t) \sin\big(\varphi_i(t)\big) + \alpha_0(t) \tag{5}$$

It is worth noting that in Eq. (1)-(3), the error signal $F(t)$ is normalized by the amplitude. This normalization is particularly effective in reducing perturbations from minor variations of amplitude on the dynamical learning of frequency and phase (Ronsse et al. 2013).

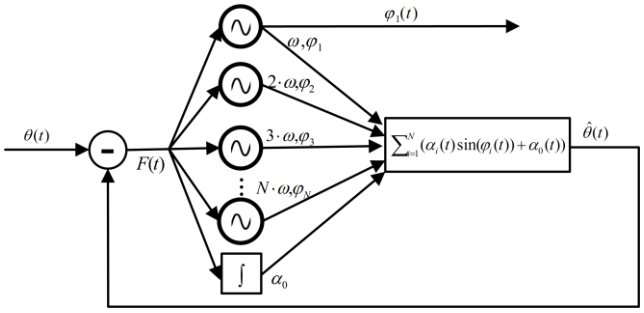

Fig. 2 Block diagram of the AO dynamic system. The input signal is decomposed into different harmonics. Phase, frequency and amplitude of each harmonic are learned by each oscillator and then used to obtain an estimation of the input signal. The error between the estimated signal (output) and the actual one (input) drives the evolution of the dynamic system.

2.1.2 Gait event detector

Kinematic and dynamic signals during walking are periodic by nature. It is thus desirable to estimate their phase by locking it to a characteristic event in each stride, so that the cycle begins at that specific instant. For instance, when the gait phase is a function of hip joint angles (HJAs), the desired gait event could be the maximum hip flexion, marked by a peak flexion angle. When the gait phase is estimated with vertical ground reaction forces (vGRF), the desired gait event could be the heel strike (HS), detected when the vGRF overcomes a certain threshold. While it is not complicated to capture these events in real time, the correctness of detection is influenced by the smoothness or dynamic features of the monitored signals. For example, a failure in detecting maximum flexion could happen if there are multiple local peaks in the joint angle profile. We could improve the performance of event detection by fusing more sensors or introducing more complex signal processing, such as

a Kalman filter. However, both methods would increase the complexity of the system or induce significant delays.

This paper conceives an alternative method to avoid possible false detections. As addressed in Subsection 2.1.1, AOs can synchronize with the frequency of any cyclic signal, providing the opportunity to estimate the current stride duration. Due to the periodicity of human gait, the desired events in two consecutive strides should be separated by an adaptive time interval in relation to the stride period. As shown in Fig. 3, if the event of k-th stride occurs at instant t_k, the next detection at time t^* is accounted as t_{k+1} only when:

$$t^* - t_k \geq \rho \cdot T(t^*) \Rightarrow t_{k+1} = t^* \quad (6)$$

where ρ is a proportional constant in the range (0,1], and $T(t)$ is the current stride period estimated with AOs, being $T(t) = \frac{2\pi}{\omega(t)}$. This means that detection at time t^* will be discarded if it happens earlier than a certain percentage of the current stride period. The expected minimum time interval is tuned with the gain ρ assumed greater than 0.5 for a normal gait, i.e. the subsequent event occurring at least after half of a period. It is worth noting that ρ equal to 1 could lead to missed valid detections due to intra-cycle variability.

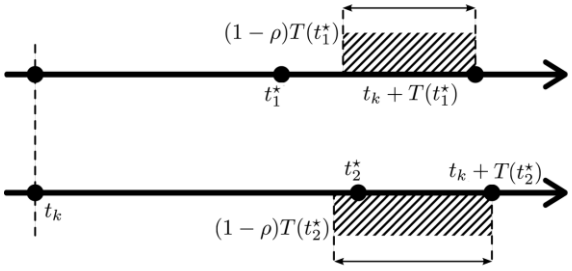

Fig. 3 Representation of the gait event detection decision algorithm: the event detected at $\boldsymbol{t_1^*}$ is discarded (too near to the last event detection), while the one at $\boldsymbol{t_2^*}$ is accepted and thus $\boldsymbol{t_{k+1} = t_2^*}$. The gain $\boldsymbol{\rho}$ tunes the acceptance threshold of stride-period variations.

2.1.3 AOs-based gait phase estimator

The gait phase $\phi(t)$ should be a variable linearly increasing from 0 to 2π rad (corresponding to 0% to 100% of stride) between two event detections. As scheduled in Fig. 1, a pool of AOs is used to acquire a continuous phase of the targeted biomechanical signal. In this subsystem, the fundamental phase $\varphi_1(t)$ learned by AOs is normalized into the interval $[0, 2\pi)$ rad and noted as $\varphi_n(t)$:

$$\varphi_n(t) = mod(\varphi_1(t), 2\pi) \quad (7)$$

According to Eq. (5), the input signal is decomposed by the AOs as a set of simple sinusoidal functions and an offset component, similarly to the performance of a Fourier transform. When $\varphi_n(t)$ equals 0 rad, the reference signal is not arbitrary but rather associated with the phase of the fundamental frequency element. Said differently, $\varphi_n(t)$ is not necessarily equal to 0 rad when the desired gait event is detected at time t_k. In order to build an accurate gait phase function, the 0-rad phase should be matched with the desired event at time t_k. Thus the phase error $P_e(t_k)$ is defined as the error between the learned phase $\varphi_n(t)$ at time t_k and 0 or 2π:

$$P_e(t_k) = \begin{cases} -\varphi_n(t_k) & \text{, if } \quad 0 \leq \varphi_n(t_k) < \pi \\ 2\pi - \varphi_n(t_k) & \text{, if } \quad \pi \leq \varphi_n(t_k) < 2\pi \end{cases} \quad (8)$$

The range of $P_e(t_k)$ is a symmetric phase interval, i.e. $[-\pi, \pi)$ rad. In particular, we observed that if $\varphi_n(t_k)$ falls within $[0, \pi)$ rad, the phase $\varphi_n(t)$ is in advance with respect to the desired phase (it reaches 2π before the next effective gait event). Conversely, if $\varphi_n(t_k)$ falls within $[\pi, 2\pi)$ rad, the phase $\varphi_n(t)$ lags behind the desired phase (it does not reach 2π at the next gait event). These two conditions are associated respectively with a negative and a positive value of $P_e(t_k)$ (see Fig. 4).

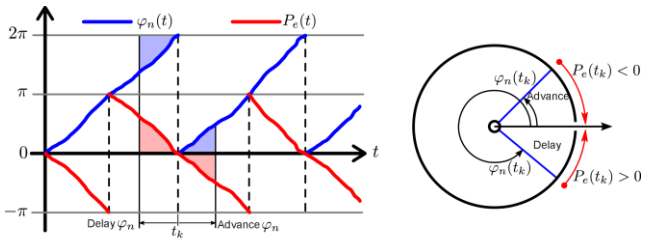

Fig. 4 From the $\boldsymbol{\varphi_n(t)}$ phase to the $\boldsymbol{P_e(t_k)}$ phase error: time-scale representation of the operation captured by Eq. (8) (left), same scheme for two particular cases of the local $\boldsymbol{t_k}$ value, being represented along a phase-circle (right). The phase error $\boldsymbol{P_e(t_k)}$ is negative/positive (clockwise/counter-clockwise direction in the right plot) if the natural phase is in advance/delay with respect to the event detection.

Some inconsistencies occur when $\varphi_n(t_k)$ fluctuates around π rad. Indeed, $P_e(t_k)$ may switch from a value close to π rad ($-\pi$ rad) to a value close to $-\pi$ rad (π rad). The big jump of $P_e(t_k)$ implies that the gait phase may vary by almost 2π rad between two consecutive strides, which is not desirable(Fig. 5).

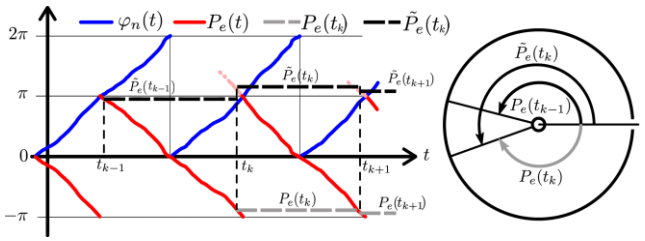

Fig. 5 From the $\boldsymbol{P_e(t_k)}$ phase to the $\boldsymbol{\widetilde{P_e}(t_k)}$ phase error. On the left, time-scale representation of the operation expressed by Eq. (8); on the right, the same representation along a phase-circle. This operation limits the sudden variations in the phase error corresponding to the gait-event detections.

To avoid such inconsistencies, the detected phase error is further updated with an equivalent 2π-shifted value $\widetilde{P}_e(t_k)$:

$$\widetilde{P}_e(t_k) = \begin{cases} P_e(t_k) - 2\pi & \text{, if } P_e(t_k) > \frac{\pi}{2} \text{ and } \widetilde{P}_e(t_{k-1}) < -\frac{\pi}{2} \\ P_e(t_k) + 2\pi & \text{, if } P_e(t_k) < -\frac{\pi}{2} \text{ and } \widetilde{P}_e(t_{k-1}) > \frac{\pi}{2} \\ P_e(t_k) & \text{, otherwise} \end{cases} \quad (9)$$

where $\widetilde{P}_e(t_k)$ keeps the same sign as its value at the previous detection. This updating only happens in the case of a jump greater than π, as illustrated in Fig. 5.

2.1.4 Phase error compensator

Based on the above analysis, the estimated gait phase can now be locked to the desired specific gait event by directly subtracting the detected phase error: $\phi(t) = \varphi_n(t) - \widetilde{P}_e(t_k)$. However, by doing so, the estimated phase $\phi(t)$ updates with an abrupt change at each event detection. The objective of this section is to propose a phase error learning mechanism that avoids this discontinuity. In addition to the AOs-based phase estimation, we introduce a novel state variable $\varphi_e(t)$ to learn $\widetilde{P}_e(t_k)$ within one stride cycle. Ideally, within the current cycle, φ_e will smoothly converge to $\widetilde{P}_e(t_k)$ as steady state. This phase error dynamic is captured by:

$$\dot{\varphi}_e = \epsilon_\varphi(t_k)\omega(t)e^{-\omega(t)(t-t_k)} \quad (10)$$

in which, $\epsilon_\varphi(t_k) = k_p[\widetilde{P}_e(t_k) - \varphi_e(t_k)]$ is the value capturing the desired variation in $\varphi_e(t)$ within one stride; k_p is a proportional gain and $\omega(t)$ is the signal frequency tracked by the AOs. Assuming that $\omega(t)$ stays constant over one period, Eq. (10) represents a first-order system filtering a fraction of the phase error at event detection. This guarantees stability and convergence of the phase error learning system.

Finally, a smooth gait phase $\phi(t)$ is obtained by subtracting φ_e from the normalized AOs phase $\varphi_n(t)$:

$$\phi(t) = mod(\varphi_n(t) - \varphi_e(t), 2\pi) \quad (11)$$

In Eq. (11), a modulo operation with 2π is applied to the corrected phase so as to bound it between $[0, 2\pi)$ rad.

2.2 Validation Experiments

The proposed gait phase estimator is validated with two different periodic biomechanical signals: HJA (hip joint angle) and vGRF (vertical ground reaction force). Both signals can be easily measured with wearable sensors. In this study, the encoder was coupled to the joint of a wearable robot and a shoe instrumented with pressure sensors, respectively. Details of the validation experiments are reported in the following parts, including the description of the experimental setup (Subsection 2.2.1), protocols (Subsection 2.2.2) and data analysis (Subsection 2.2.3).

2.2.1 Experimental setup

The gait phase estimator was validated with walking subjects wearing an active pelvis orthosis and a pair of instrumented shoes (see Fig. 6), both developed at The BioRobotics Institute, Scuola Superiore Sant'Anna, Italy.

The active pelvis orthosis is a light-weight exoskeleton capable of assisting bilateral hip flexion-extension movements (Giovacchini et al. 2014). This orthosis guarantees compliant interactions with the human leg in a zero-torque mode without hindering the user's voluntary movements, since the actuation principle is based on series elastic actuators (Pratt and Williamson 1995; Veneman et al. 2006). Its controller is implemented on a cRIO board endowed with a field programmable gate array (FPGA) and a NI processor running LabVIEW2011 RT module (National Instruments, Austin, Texas) at a frequency of 1 kHz (Giovacchini et al. 2014). In the exoskeleton system, the subject's HJAs are measured by absolute encoders mounted on the robotic joint side which we consider for the purpose of the study to be aligned with the human hip articulation.

During ground-level walking, the hip joint follows a quasi-sine-wave trajectory. Each stride cycle therefore can be easily distinguished with the maximum HJA, i.e. the maximum flexion position. In our experiment, the maximum HJA was detected when the difference between the current angle and the previous angle changed from positive to negative. This event detection was supervised by Eq. (6). Moreover, we also defined that the maximum HJA $\theta(t)$ should comply with $\theta(t) \geq \alpha_0(t) + \beta \cdot \alpha_1(t)$, where $\alpha_0(t)$ and $\alpha_1(t)$ were the offset and amplitude respectively learned by AOs with β being a constant within [0, 1]. This windowing guaranteed acceptance of the detection of the positive peak close to the maximum flexion position. Thanks to the high sampling frequency of the controller (1 kHz), there was only 1 ms of event detection delay.

On the other hand, the pair of sensitive insoles of the instrumented shoes was composed of a matrix of 64 optoelectronic sensors that recorded plantar pressure distribution. Communication between the shoes and the LabVIEW RT controller was through a Bluetooth protocol. The shoes measured both vGRF and the position of the centre of pressure (CoP) (Crea et al. 2014; Donati et al. 2013). During the stance phase, the CoP signal was delivered as a real-finite number, while during the swing phase, the CoP was represented by a Not-a-Number. In our experiments, when the gait phase was estimated with vGRF, HS was selected as the desired gait event. It was detected only when the CoP of one limb changed from a Not-a-Number to a real-finite number and the CoP of the other leg was also a finite value. This allowed the HS to be detected always during the double support phase. Furthermore, detection had to be consistent with the condition in Eq. (6).

In the LabVIEW RT controller, the gait phase estimator tracked the HJA and vGRF in parallel with two separated pools

of AOs. For simplicity, the left and right gait patterns were considered as symmetric (at least for the healthy subjects tested in this study), so that only the right or left gait phase was estimated and the contralateral gait phase was computed as $mod((\phi(t)+\pi), 2\pi)$.

To improve the stability and accuracy of the estimated gait phase for both limbs, the error signal $F(t)$ for HJA-based AOs was calculated by fusing the signals from both left and right limbs:

$$\hat{\theta}_L(t) = \sum_{i=1}^{N} [\alpha_i sin\varphi_i(t) + \alpha_0(t)] \quad (12)$$

$$\hat{\theta}_R(t) = \sum_{i=1}^{N} [\alpha_i \sin(\varphi_i(t) + \pi \cdot i) + \alpha_0(t) \quad (13)$$

$$\dot{\omega} = \frac{\nu_\omega}{\sum \alpha_i} \cdot [F_L(t)\cos(\varphi_1(t)) + F_R(t)\cos(\varphi_1(t)+\pi)] \quad (14)$$

$$\dot{\alpha_\iota} = \eta \cdot [F_L(t) sin\varphi_i(t) + F_R(t) sin(\varphi_i(t) + \pi \cdot i)] \quad (15)$$

$$\dot{\alpha_0} = \eta \cdot [F_L(t) + F_R(t)] \quad (16)$$

where $\hat{\theta}_L(t)$ and $\hat{\theta}_R(t)$ were the estimated left and right hip joints respectively. The left HJA phase learning was still governed by Eq. (1). As noted in the above equations, the teaching signal of oscillators $F(t)$ was synthesized with the errors from both left and right HJAs, namely $F_L(t)$ and $F_R(t)$. When speed was changed, the symmetric feature of HJA during speed transition was violated, so $F(t)$ increased and accelerated the update of state variables. On the other hand, the greater variation also implied less accuracy.

Due to the limited homogeneity in the fabrication of the sensorized insoles, vGRF signals measured from left and right shoes had different amplitudes. We only used the left insole signals in our experiments, i.e. $F(t)$ was calculated as the error from left vGRF. The AOs dynamic system was as depicted in Eq. (1)-(5).

All parameters in the AOs dynamic system with HJA and vGRF were tuned by experience and preliminary trials. Values were selected by searching for a trade-off between the initial learning speed and the smoothness at steady state. In this study, the parameters for HJA tracking were selected as $N = 3, \nu_\varphi = 1, \nu_\omega = 1, \eta = 0.4$ to tune the number of harmonics, phase, frequency and amplitude learning speeds respectively. While in the vGRF learning process, the parameters were set as: $N = 5, \nu_\varphi = 4, \nu_\omega = 4, \eta = 1.6$. With these parameters, the periodic signals could be synchronized in a short time (within 7 strides). To determine a proper phase error learning gain k_p in Eq. (10), we ran several simulations before the real experiments with values in the range of [0.1, 2]. Taking k_p equal to 0.5 gave the smallest phase error and was therefore kept for all experimental sessions. The timing parameter ρ in the event detector was set to 0.7 for both HJA and vGRF, which were found to cause neither multi nor missed detections over one stride in the preliminary trials.

2.2.2 *Experimental protocols*

Two experimental sessions were designed, namely treadmill and ground-floor walking in an ecological environment.

Six healthy subjects, aged between 24 and 32 years, participated in the first experimental session. Each subject was asked to walk on a treadmill at different speeds, wearing the pelvis orthosis in zero torque mode and the pair of sensorized shoes. State vectors of AOs ($\varphi_n(t), \omega(t)$), phase reset error $\widetilde{P_e}(t_k)$, estimated gait phase $\phi(t)$, and the input signals, i.e. HJAs, vGRFs, and CoPs were recorded online.

Data recording was initiated when a subject stood still on the treadmill. After 10 seconds, the subject started walking at 2.4 km/h (0.67 m/s). The speed was smoothly increased every two minutes by 1.0 km/h within 10 seconds until reaching 4.4 km/h (1.22 m/s). Then from 4.4 km/h the speed was smoothly decreased by 1.0 km/h every two minutes (in a time interval of 10 seconds) until returning to the starting speed (2.4 km/h). After 2 minutes at 2.4 km/h, the subject suddenly stopped walking and stood on the treadmill, while data was acquired for another 10 seconds. Each time the speed was changed, the experimenter triggered a flag signal manually from the control interface to mark the beginning and ending time of speed transition. When subjects walked on the treadmill, they were allowed to hold the handrails just for keeping balance and for safety reasons.

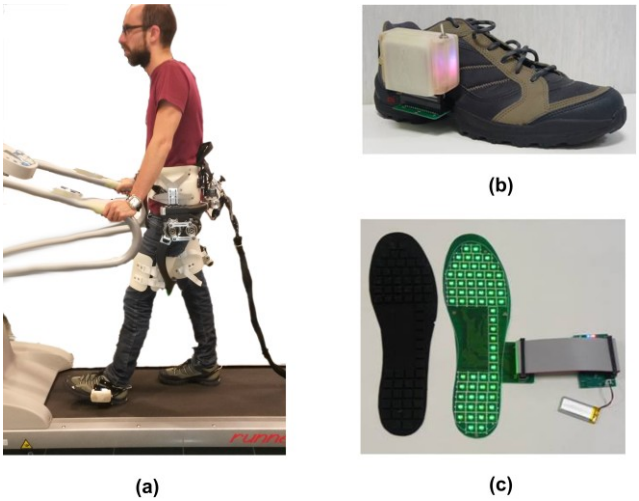

Fig. 6 Experimental setup. Subjects walked on a treadmill wearing (a) an active pelvis orthosis and (b) a pair of shoes instrumented with (c) sensitive plantar pressure insoles.

One of the subjects (24 years old, weight 60 kg, height 1.73 m) additionally took part in the free walking session. During this session, only vGRF was tracked by the gait phase estimator as the pelvis orthosis could not work without wired power supply and communication. The walking distance of the subject was also limited by the Bluetooth communication protocol. Finally, the subject was asked to walk over a distance of ten meters only wearing the shoes. Three trials were completed and each trial lasted 3 minutes. To test various walking conditions,

the subject was asked to randomly walk at his self-selected slow, normal and fast speeds in each trial. During the experiment, state vectors of AOs, phase error $\widetilde{P_e}(t_k)$, estimated gait phase ϕ(t), and the input vGRFs and CoPs were recorded.

2.2.3 Data Analysis

During the post-processing phase, all the recorded data sets, including gait phases $\phi(t)$, were segmented into each stride cycle by referring to the detected gait events. Data sets collected from treadmill walking were also divided into constant speeds and speed transitions from the manually triggered flags.

As a first analysis, the linearity of the gait phase was evaluated. An ideal gait phase is expected to increase linearly within one stride. The linearity of a signal can be represented by a constant of the instantaneous slope, i.e. a constant of the first derivative. So the standard deviation of the first derivative of the estimated gait phase $\frac{d\phi(t)}{dt}$ was computed for each stride.

Then, a benchmark gait phase was built to quantify the accuracy of the estimated gait phase in a gait cycle. A variable linearly increasing from 0 to 2π rad between the beginning and end of a stride was considered. If the stride period of the k-th stride was $T_k = t_{k+1} - t_k$, the benchmark phase was created as $\varphi_{lin}(t) = \frac{2\pi}{T_k} \cdot (t - t_k)$, with $t \in [t_k, t_{k+1})$. The phase error within one stride was calculated by subtracting $\varphi_{lin}(t)$ from $\phi(t)$; before this, however, $\phi(t)$ needed to be adjusted to keep consistent with $\varphi_{lin}(t)$ in one stride. The final subtraction operation was performed between $\varphi_{lin}(t)$ and the adjusted gait phase $\varphi_g(t)$:

$$\varphi_g(t) = \begin{cases} \phi_k(t) - 2\pi \text{ if } \pi \le \phi_k(t) < 2\pi, t \in [t_k, t_{\phi_k(t)=0}] \\ \phi_{k+1}(t) + 2\pi \text{ if } 0 \le \phi_{k+1}(t) < \pi, t \in [t_{\phi_{k+1}(t)=0}, t_{k+1}) \\ \phi_k(t) \end{cases}$$

Besides the average errors from all strides along one stride cycle, we also evaluated the phase estimation performance at the desired gait events. Therefore, the root mean square error (RMSE) of $\varphi_g(t)$ with respect to $\varphi_{lin}(t)$ at time t_k, namely the residual phase error $P_{ge}(t_k)$, was computed. The analyses were carried out for both treadmill walking (constant-speed and speed-transition) and ground-floor free walking. In treadmill walking, ANOVA and t-test were performed in order to assess whether the results were significantly affected by the walking speeds, speed increase and decrease, or the tracked biomechanical signal.

The results of our method were also benchmarked against two methods from the literature. One was proposed by Lenzi et al. (2013), hereafter called the Lenzi method. In each gait cycle, their gait phase $\varphi_{lz}(t)$ was estimated based on the frequency learned by AOs. For instance, in k-th stride, the phase was defined as $\varphi_{lz}(t) = \omega(t) \cdot t\_k, t\epsilon[t_k, t_{k+1}), t\_k\epsilon[0, t_{k+1} - t_k)$. The other method was proposed in (Lewis and Ferris 2011), hereafter called the Ferris method. In their method, the expected stride period was estimated by averaging the durations of ten previous strides. For the k-th stride, the gait phase evolved as $\varphi_{fs}(t) = \bar{\omega}_{10} \cdot t\_k, t\epsilon[0, t_{k+1} - t_k)$. The gait phase $\varphi_{lz}(t)$ and $\varphi_{fs}(t)$ were obtained by off-line processing with the recorded HJA or vGRF, as well as the corresponding phase errors. It is worth pointing out that the phase errors from these two methods are 0 rad at time t_k. This is due to the definition of both phase estimators, which always starts from 0 rad at the beginning of a stride and evolves as the defined equations. Then, at the next event detection, whatever the phase value is, it is suddenly reset to 0 rad. In the data analysis, the error between 2π and this stride-end phase (the k-1-th stride simulated using the Lenzi and Ferris methods) was compared to $P_{ge}(t_k)$. This was equivalent to the stride-end error of the k-1-th stride due to the continuity of our AOs-based phase. An inferential statistical t-test was run to compare the results from these three methods.

All offline data analysis and statistics were performed with Matlab (version R2012a, The MathWorks Inc, Natick, MA).

3 Results

3.1 Ground-level walking on treadmill

This section presents the data analysis results from the first experimental session. First of all, out of the data collected from each subject, there were neither multiple nor missed event detections within one stride, except for one missed detection found among 418 strides (from subject #4), 408 strides (from subject #5) and 489 strides (from subject #6) respectively, in the case of vGRF-based estimation. The missed detections were then added off-line to segment the data sets.

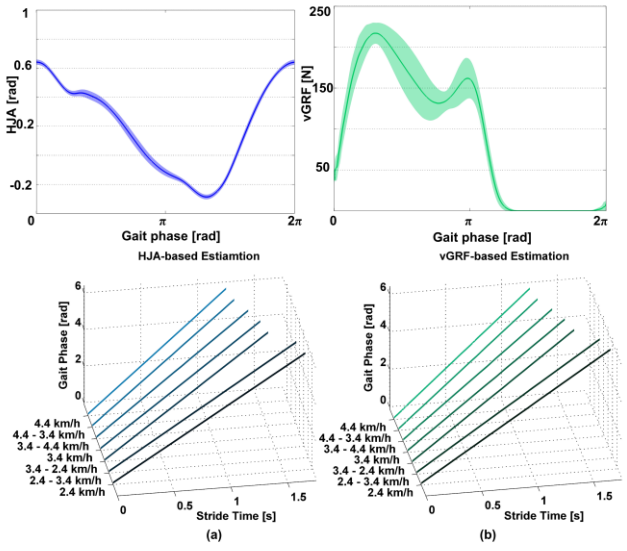

Fig. 7 Gait phase detection based on AOs coupled with HJA (a) and vGRF (b). The upper graphs show the average bio-mechanical signal (solid line) input to the AOs, along with its standard deviation contour (shadowed line) segmented for each gait cycle. The lower graphs report the averaged gait phases under different walking conditions.

The upper two plots in Fig. 7 display the average HJA and vGRF of one subject during all walking conditions. Both of them were segmented with the detected gait events. The shadow areas in the two plots represent the standard deviations of HJA and vGRF, which are 0.05 rad (5% of the range of movement of HJA) and 5 N (2% of the maximum vGRF) at the starting point. These limited variations supported the reliability of our gait event detection system.

The lower two graphs in Fig. 7 display the average gait phase $\varphi_g(t)$ obtained from one subject under different walking conditions. Generally, the gait phase could linearly increase from around 0 rad to 2π rad in one stride cycle. The quantitative assessment of linearity reports that the first derivative of $\varphi_g(t)$ is lower than 0.0005 rad/ms for all strides during constant speed and speed transition walking. This result illustrates the linearity of the estimated gait phase within one stride.

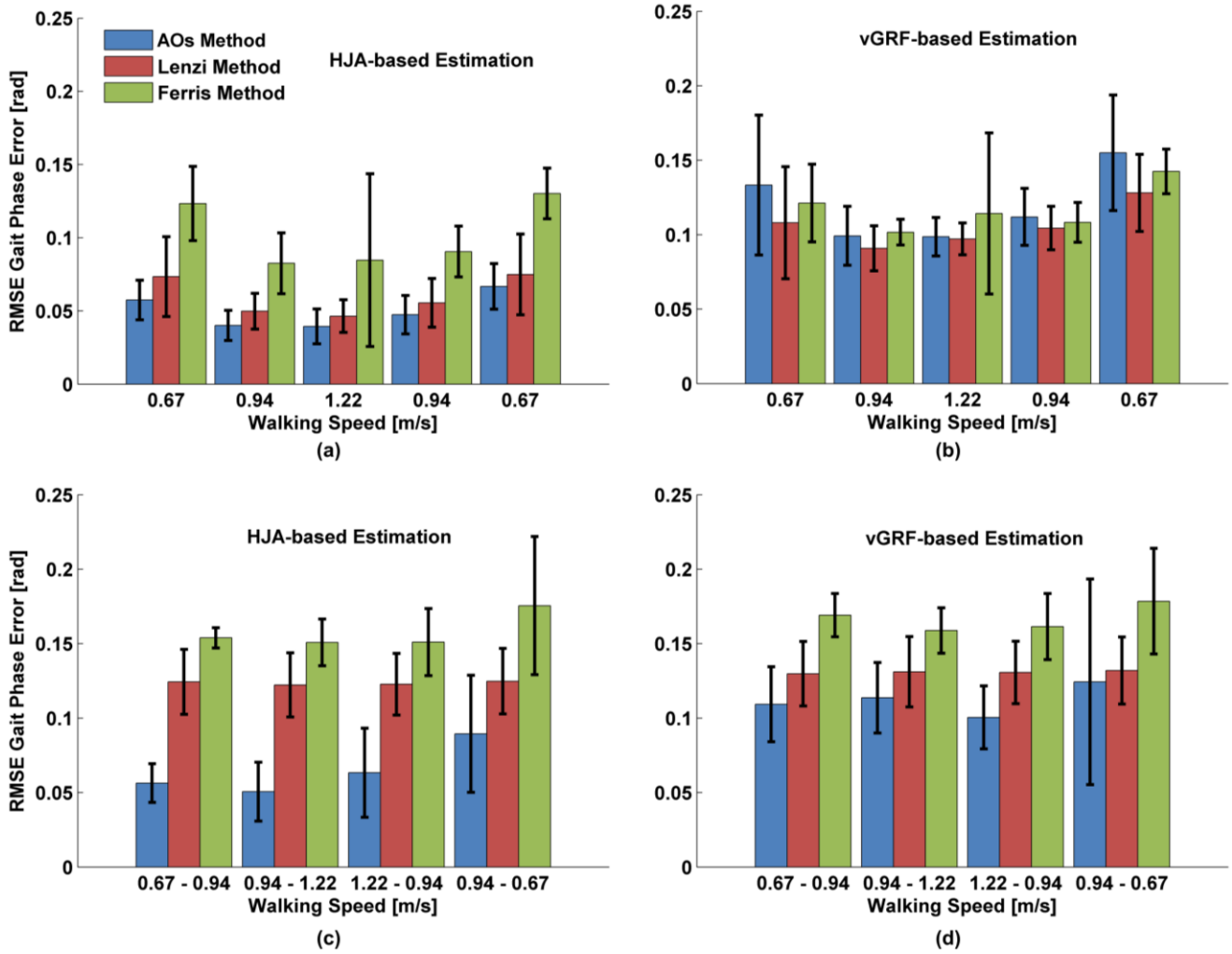

Fig. 8 Averaged RMSE of the residual phase error at the desired gait event. Data is taken from all subjects. Each graph reports the error returned from the three compared methods under different conditions. The upper graphs report the results under constant-speed walking coupled with the HJA (a) and vGRF (b). The lower graphs report the results under speed-transition walking coupled with the HJA (c) and vGRF (d).

3.1.1 Gait phase error at the desired gait event

The performance of the AOs-based gait phase estimator at the desired gait event, while subjects walked on the treadmill, is shown in Fig. 8. The averaged RMSEs of $P_{ge}(t_k)$ acquired with HJA and vGRF, during constant speed walking, are presented in Fig. 8(a) and (b) respectively. The results of one-way ANOVA analysis show that the errors at different speeds are not significantly different ($p = 0.02$ for HJA, $p=0.11$ for vGRF). In Fig. 8 (a), the maximum averaged RMSE of $P_{ge}(t_k)$ is 0.067 rad, equivalent to 1.1% of one stride cycle. The standard deviation of RMSE is kept below 0.016 rad in all four conditions, providing evidence of the stability of a HJA-based gait phase estimator. However, all errors are higher with vGRF being the reference signal for estimating the gait phases

($p<0.05$ from all paired t-test of errors with HJA and errors with vGRF at the same speed). As displayed in Fig. 8 (b), the RMSE of $P_{ge}(t_k)$ maximally rises to 0.155 rad at the slowest walking condition (i.e. 0.67 m/s). The maximum standard deviation of RMSE also increases to 0.047 rad. We assume this is due to the vGRF signal being more complex than the HJA signal, which would require the AOs to learn the dynamics of a greater number of harmonics. In the event of non-optimal parameters for AOs, the phase and frequency learning would be affected by more variations.

The phase errors of HJA-based and vGRF-based estimations while subjects were changing their walking speeds are those plotted in Fig. 8 (c) and Fig. 8 (d), respectively. The estimated gait phases are less accurate and more variable than during constant speeds. For instance, the maximum RMSE of $P_{ge}(t_k)$ reaches 0.090 ± 0.039 rad with HJA (Fig. 8 (c)) and 0.124 ± 0.069 rad with vGRF (Fig. 8 (d)). There is no statistical difference between speed increasing and decreasing errors (ANOVA: $p=0.10$ for HJA, $p=0.79$ for vGRF). However, similarly to the results of constant speed walking, the phase errors of vGRF-based estimation are higher than HJA-based estimation ($p<0.05$ for all paired t-test except $p=0.22$ when the speed decreases from 0.94 to 0.67 m/s).

In order to statistically analyze the difference of $P_{ge}(t_k)$ from constant-speed walking and speed-transition walking, a one-way ANOVA analysis was implemented. Results show that in the case of HJA, RMSE of $P_{ge}(t_k)$ significantly increases when speed changes ($p=0.004$) while with vGRF, it remains identical under all walking conditions ($p=0.14$). This could be explained by the fact that the dynamics of AOs tracking HJA was updated with a bilateral error signal, whereas a monolateral error signal was used for the dynamics of vGRF. While the speed was changing, the asymmetry between left and right gait pattern caused more variations to the dynamics of HJA leading to less accuracy in phase estimation.

Fig. 8 also shows the gait phase errors in simulations using the Lenzi Method and Ferris Method. At constant speeds (in Fig. 8 (a) and (b)), the maximum RMSEs using the Lenzi method are 0.075 ± 0.028 rad for HJA detection and 0.128 ± 0.026 rad for vGRF based detection, while the maximum RMSEs using the Ferris method are 0.130 ± 0.017 rad for HJA detection and 0.142 ± 0.015 rad for vGRF based detection. When the speed is changing (in Fig. 8 (c) and (d)), the RMSEs using the Lenzi method are 0.125 ± 0.022 rad for HJA detection and 0.132 ± 0.026 rad for vGRF based detection; while the RMSEs using the Ferris method are 0.176 ± 0.046 rad for HJA detection and 0.179 ± 0.036 rad for vGRF based detection.

Based on the above results, the AOs method shows better performance than the other two methods except for the estimation with vGRF at constant speeds (see Fig. 8 (b)). In this case, the Lenzi method shows lower phase residual errors than our AOs method (t-test: $p<0.05$ at 0.67 m/s), and there is no significant difference between the AOs method and Ferris method ($p>0.05$ at all speeds).

3.1.2 Phase error within one stride cycle

To quantitatively validate the accuracy of the estimated gait phase within one stride cycle, the error between estimated phase $\varphi_g(t)$ and benchmark phase $\varphi_{lin}(t)$ was plotted, as shown in Fig. 9.

Firstly, the performance of the gait phase estimation of our AOs-based method is presented in Fig. 9 (a) and (b). In the case of HJA, a maximum phase error is found when the speed is increased from 0.67 to 0.94 m/s: 0.085 rad at 76% of stride (see Fig. 9 (a)). With vGRF, the maximum phase error is -0.117 rad at 44% of stride when the speed is decreased from 0.94 to 0.67 m/s (see Fig. 9 (b)). Consistent with the results at the desired gait event (Fig. 8), errors within one stride are higher when the speed varies rather than when the speed is constant, particularly with vGRF. This is mostly due to the fact than when the speed changes, there are larger variations in the tracked signals as well. Consequently, the oscillators adapt their state variables, which leave steady-state regime. Nevertheless, thanks to the adaptive phase error learning mechanism, these errors are dynamically compensated and converge back to zero at the end of each stride, for example, maximally reaching 0.045 rad with HJA and and 0.061 rad with vGRF (see Fig. 9 (a) in Fig. 9 (b)).

The phase estimation errors within one gait cycle simulated with the Lenzi and Ferris methods are reported in Fig. 9 (c)-(d) and Fig. 9 (e)-(f), respectively. As expected, due to its adaptive stride duration, the overall performance of the Lenzi method is similar to ours. Its maximum phase error with HJA is -0.087 rad at 68% of stride when the speed slows down from 0.94 to 0.67 m/s (see Fig. 9 (b)). In the case of vGRF, the maximum phase error is 0.104 rad at 52% of stride when the speed rises from 0.67 to 0.94 m/s (see Fig. 9 (b)). However, due to the absence of error learning and compensation, their gait phase continues to be over- or under- estimated in one stride, as illustrated in Fig. 9 (d).

The results shown in Fig. 9 (e)-(f) suggest that when speed is changing, the Ferris method causes much higher errors than the other two methods, maximally being 0.438 rad with HJA and 0.407 rad with vGRF. In particular, if the speed accelerates, the error increases positively, so that the gait phase is underestimated. On the contrary, if the speed decelerates, the error increases negatively, so that the gait phase is overestimated. This is due to the delay in updating stride duration when the speed changes. However, when speed is constant, the phase errors are quite small, i.e. below 0.017 rad out of results with both HJA and vGRF.

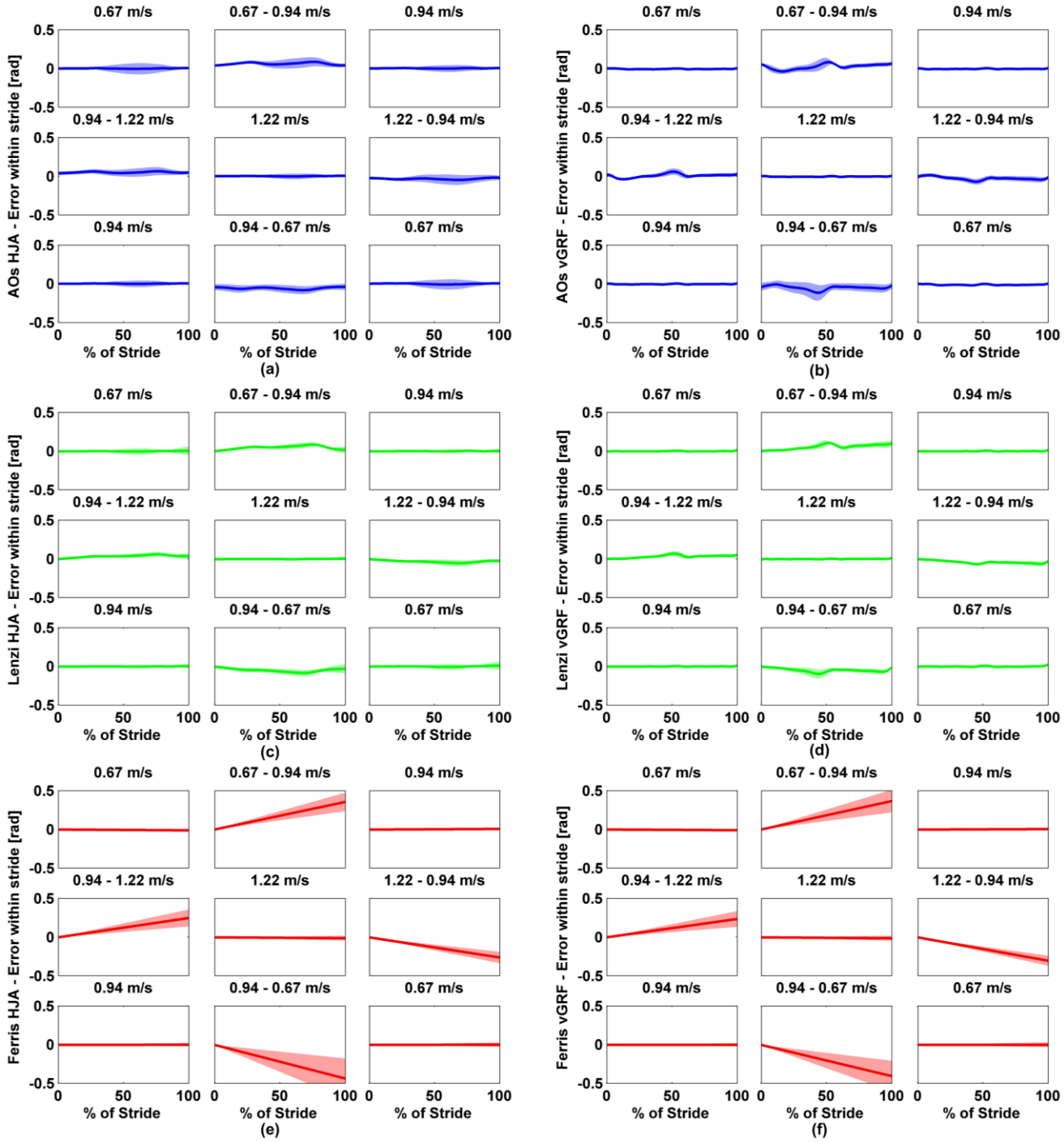

Fig. 9 Gait phase errors within one stride cycle in all walking conditions. In each graph, the solid line stands for the averaged value of all six subjects, while the shadow represents the standard deviation. Graphs (a) and (b) respectively report the results of AOs method tracking HJA and vGRF; graphs (c) and (d) respectively report the results of the Lenzi method simulating with HJA and vGRF; graphs (e) and (f) respectively report the results of the Ferris method simulating with HJA and vGRF.

In order to evaluate the continuity of the estimated gait phase at stride transition, we compared the phase errors at 0% of stride and 100% of stride. This evaluation schedule underlies that the gait phase difference at stride transition represented by a percentage of the whole stride (2π) should be consistent with the intra-cycle variability of human walking over one stride (Bollens et al. 2014).

The phase differences found at stride transition are presented in Table 1. With the AOs-based estimator, the maximum phase difference is 0.009 rad out of all walking conditions except for the eighth plot of Fig. 9 (b) – which slows down from 0.94 to 0.67 m/s with vGRF – being 0.020 rad. When using the Lenzi and Ferris methods, the phase difference increases, as demonstrated in both Table 1 and Fig. 9 (c)-(f). The differences

between the phase at the end of the stride and at the beginning of the next stride could reach 0.096 rad with the Lenzi method and -0.438 rad with the Ferris method, especially when speed changes. This reveals that the variations of the estimated gait phase at stride transition are 1.5% and 7.0% respectively, which are both much higher than the 0.3% estimated with our AOs method.

Table 1 Maximal phase difference between the end of the stride and the beginning of the next stride in all walking conditions.

		Maximum phase difference [rad]	
		Constant speed	Speed transition
HJA-based estimation	AOs	0.006	0.007
	Lenzi	0.007	0.034
	Ferris	-0.016	-0.438
vGRF-based estimation	AOs	0.004	0.020
	Lenzi	0.024	0.096
	Ferris	-0.017	-0.407

3.2 Free walking

This section reports the residual phase error at the desired gait event during the second experimental session, namely level-ground free walking mode. As explained in Subsection 2.2.2 *Experimental Protocols,* because of the portability limitation of the pelvis orthosis, only vGRF was used to validate the gait phase estimator. Thus only the averaged RMSE of the phase error with vGRF was calculated for each trial and presented in Table 2. Results simulated with the Lenzi and Ferris methods are presented in Table 2 as well.

Table 2 Average RMSE of residual phase error $P_{ge}(t_k)$ resulting from the AOs, Lenzi and Ferris methods under three free-walking trials**.**

	Averaged RMSE of residual phase error [rad]		
	AOs	**Lenzi**	**Ferris**
Trial 1	0.278	0.477	0.548
Trial 2	0.267	0.242	0.460
Trial 3	0.221	0.205	0.474
Averaged	0.255	0.308	0.494
Std. Dev.	0.030	0.148	0.047

Compared to the results in Fig. 8, the phase errors at the desired gait event using all three methods are generally higher in the free walking trials. In particular, the error resulting from our AOs maximally reaches 0.278 rad, while it reaches 0.477 rad with the Lenzi method and 0.548 rad with the Ferris method. During the first free walking trial, the AOs method demonstrated better accuracy in estimating the gait phase. Its phase residual error is 0.169 rad less than the Lenzi method and 0.270 rad less than the Ferris method. Conversely, in Trial 2 and Trial 3, there was no significant phase residual difference between the AOs method and the Lenzi method, i.e. about 0.02 rad in both cases. The difference among the three trials could be due to the more gentle speed transition in the first trial than in the other two trials.

4 Discussion

4.1 Performance of the gait phase estimator

We presented a novel algorithm based on AOs in this work for the purpose of acquiring an accurate and continuous gait phase during walking. Through two validation sessions, the gait phase estimator proved to be useful in both treadmill walking and free walking experimental environments. In particular, the gait phase was estimated by means of two commonly used biomechanical signals which are usually measured in exoskeleton systems: HJA and vGRF.

Human walking biomechanics is implemented by lower-limb muscular activities organized by a series of motor primitives (Cappellini and Ivanenko 2006). Consequently, any variation in steady-state locomotion is not abrupt and follows a specific phase-dependent pattern. In our gait phase estimator, a residual phase error was calculated at each event detection. It captured the inherent fluctuations of walking. At the start of the current stride, the identified phase error captured whether the phase estimation was in delay or anticipation. Then, a phase error learning mechanism was designed to smoothly compensate this error within the current stride cycle. The results of the treadmill tests proved that by using this method the RMSE of the phase error at the desired gait event was always less than 2.5% of stride with both signals. In the free walking tests, only vGRF was tracked, and the maximum RMSE was 4.4 % of stride at the desired HS. In general, the phase error with vGRF was higher than with HJA (see Fig. 8 and Fig. 9). Indeed, the profile of vGRF has more harmonics than the quasi-sinusoidal profile of HJA. In fact, in this study, we set 5 harmonics for vGRF and 3 for HJA. Moreover, it is also difficult to find a set of parameters for the AOs in order to improve the accuracy of tracking vGRF and obtain a smooth estimation of its dynamics. An offline simulation study showed that the accuracy of estimated gait phase in steady sate would not significantly improve when the parameters for phase, frequency and amplitude learning being increased/decreased by the same percentage. For instance, the average RMSE of residual phase error from vGRF was kept being 0.15 rad when $(\nu_\varphi, \nu_\omega, \eta)$ changed from (4, 4, 1.6) to (2, 2, 0.8) and (8, 8, 3.2) respectively. However, when the parameters were larger, the learned frequency was noisier implying larger phase variability. In contrast, when the parameters were too small, it took longer time to adapt to new gait pattern. Then, if ν_φ, ν_ω were kept the

same but η was increased twice, the steady state error did not change significantly but the frequency was affected by high variability and vice versa. This exactly represents one of the limitations of our approach: several parameters have to be tuned by trial and error to achieve the more suitable performance for this case of study. This could also partly explain the increased phase error during speed transitions and free walking. Another possible reason for the higher error with vGRF is the stability of sensorized insoles in measuring foot pressures. The envelope of the vGRF may mildly vary between strides due to different foot contacting positions on the insoles. As a result, more variations would be tracked during the dynamic learning of the phase and frequency, further affecting the accuracy of the gait phase estimation.

The results of our proposed method were also compared with two well-known gait phase estimation methods from the literature, called Lenzi method and Ferris method. We found that during constant-speed walking, these three methods were all able to accurately estimate the gait phase within the gait cycle, especially considering the phase error Fig. 9. However, when subjects were changing their walking speed, both our method and the Lenzi method showed better adaptability during phase estimation. For example, when using HJA, the maximal phase error within one stride resulting from the AOs method was 1.8% of stride and 1.6% of stride with the Lenzi method, while the Ferris method could reach 7.0% of stride maximally. Both our method and the Lenzi method achieved a dynamic learning of the gait frequency with AOs, so that stride duration was constantly updated during the cycle. Contrarily, in the Ferris method, stride duration was only updated at the desired gait event by averaging the durations of the ten previous strides. As a result, the estimated gait phase was governed by a much slower adaptation.

Here, it is also worth noting that even though the accuracy of our method is only 0.2% higher than the Lenzi method, our gait phase has the advantage of better adapting to speed changes. According to Eq. (1), the evolution of phase variable in our estimator was not only driven by the learned frequency but also by the variation in frequency $\dot{\omega}(t)$ (equivalent to the item $\nu_\varphi \frac{F(t)}{\sum \alpha_i} \cos\big(\varphi_i(t)\big)$ in Eq. (1)). Therefore, the gait phase estimation also implies the tendency of gait changing, i.e. acceleration or deceleration.

Additionally, our method also benchmarked its continuity of phase estimation at stride transition unlike both Lenzi and Ferris methods (see Table 1). In the proposed AOs-based estimator, the phase is not suddenly reset to 0 rad upon the detection of the desired event. In contrast, a phase error is computed and used to update a dynamic state variable, the latter being in turn subtracted from the gait phase estimate. Therefore, phase resetting follows a smooth dynamical behavior. Oppositely, in both the Lenzi and Ferris methods, the gait phase in each stride was forced to zero which means that the phase was abruptly reset to zero once a desired gait event was detected regardless of its current value. Even though such kind of forcible phase reset ensured accuracy at the beginning of the stride, a phase jump was also generated between the end of the previous stride and the beginning of the current stride. Hence, despite the continuity within one stride, the gait phase was not continuous between each cycle of the locomotion task.

4.2 Usability for providing assistance

The proposed method of walking phase estimation could be a useful tool in the design of strategies for lower-limb assistive orthoses. It is possible to design and generate online a smooth torque profile or joint trajectory as a function of the gait phase. The timing of the desired torque or trajectory profiles can be finely tuned to conceive subject-specific assistance and optimize the assistive benefits. Potentially, the exoskeleton could augment the residual voluntary mobility of the elderly or individuals affected by mild impairments. On the other hand, the gait phase also provides the opportunity to tune the assistance by referring to biomechanics databases which are usually reported as a function of gait phase. For instance, assistance can be tuned according to relevant muscles activities, given the evidence of motor primitives organized in a phase-dependent fashion.

Some assistive strategies can also be conceived by interpolating the torque profile or joint trajectory reported in the literature (Lenzi et al. 2013). In this case, the gait phase estimate is especially required to be accurate and continuous both within and between strides. If we consider the ankle torque during the push off phase, a phase error or phase jump of 2% of stride corresponds to an error of 0.1 N·m/kg, equivalent to almost 7 N·m for a 70-kg person. An abrupt transition of 7 N·m may overload the user both mentally and physically, or even be perceived as painful if the user is in fragile health conditions. In the control of a transfermoral prosthesis, 2% of stride difference could also bring an error of 6.5 deg for the knee joint angle during the swing phase. The mistaken knee position could lead to improper foot clearance if the knee is not sufficiently flexed. An abrupt transition of 6.5 deg, if the phase is not continuous, may also disturb balance during amputee walking. Therefore, in the control of some specific gait events, even if the phase accuracy is improved by only 1% of stride duration, it can be critical for safety considerations.

Finally, our AOs-based gait phase estimator also proved to be reliable in a free walking scenario. This illustrates that the proposed methodology offers a reliable assistive approach for the use of a portable assistive device in an ecological environment. Given the results achieved in the free walking trials, we can also expect promising results in estimating other

periodical locomotion activities, such as stair climbing and slope walking.

4.3 Extension to other sensory systems

The method proposed by (Holgate et al. 2009) derived a phase estimator from the profile of the tibia angle. In contrast, our AOs-based gait phase estimator can acquire a continuous and accurate gait phase from any periodic biomechanical signal. Its implementation can be divided into three steps: a primary phase estimation based on AOs, desired gait event detection and phase error compensation. All three steps require very few computations (actually, about one line of code corresponding to each of the equations in this paper) and have no particular requirements for the profile of the periodic signal or the desired gait event.

In this study, our methodology was validated through two commonly used signals, HJA and vGRF, and by means of a lower-limb assistive orthosis and instrumented shoes. Nevertheless, the phase estimator can be integrated to other sensory systems. For instance, it can track a filtered electromyography signal if the muscle is activated cyclically. In such a case, the desired biomechanical event could be the onset of muscle contraction, represented by the onset of the linear envelop of the electromyographic signal. This is particularly useful if the gait phase wishes to be synchronized with a specific muscular activity.

Due to the continuity and adaptivity of our phase estimator, the zero gait phase can be associated with any desired biomechanical event. For instance, when the phase is tracking the vGRF, the desired gait event could also be the toe off. In this case, the gait phase would increase from 0 to 100% of stride between two consecutive toe-off detections.

Furthermore, by combining the feedback (from the sensory system) and feedforward (rhythmicity of AOs) information, the estimated gait phase can still evolve continuously in the case of event detection failure, so that assistance can be delivered continuously. A consequence is that no phase error is detected at stride beginning, causing the reduction of estimated gait phase accuracy. On the other hand, if the sensor fails to provide input signal, the sensory failure can be detected and the assistive action can be progressively switched off. During this transition period, the AOs would still provide a continuous reference for the gait phase, based on the previous cycles. This would provide a more graceful degradation of assistance rather than the instantaneous shutting down of the device in case of failure. Such a scenario would be perceived as a strong disturbance for the wearer, mainly if the assistive level is high.

4.4 Limitation of this study

As discussed in Subsection 4.1, the new algorithm developed to estimate the gait phase is sensitive to the tuning of the AOs parameters, especially for a signal with several harmonics. Therefore, different parameters may change the results. In this study, the parameters were tuned by experience and we found that the vGRF was not tracked with the same accuracy as HJA. In order to circumvent this problem, an automated parameter optimization would have to be provided.

Another limitation of this work is that the validation activities were restricted to subjects with healthy gait patterns. An abnormal gait pattern, e.g. the gait of post-stroke patients, would bring more instability to the synchronization of AOs. Even if it is possible to capture the fundamental phase and frequency features during steady walking, any unexpected movement would cause more variations to the phase estimation, resulting in failure of the potentially provided assistance.

5 Conclusions

A novel online AOs-based gait phase estimator was presented in this paper. The algorithm relied on the intrinsic adaptive properties of AOs for extracting the main features of a periodic signal (phase, frequency, amplitudes and offset). The fundamental phase of a wearable sensor signal learned by the AO dynamical system was normalized into $[0, 2\pi)$ rad to represent the phase of one stride cycle. The error between the normalized phase and a desired phase (ideally 0 rad at the desired gait event) was calculated and learned dynamically, being triggered by an event detection block. Then the desired gait phase was calculated in real time by subtracting the learned error from the AOs phase in a smooth and dynamic manner. This solution provided an accurate and continuous estimation of the gait phase during human walking without involving a complex sensory apparatus. The performance was validated with two experimental sessions carried out with two different walking-related cyclic signals: HJAs and vGRFs. Six subjects were recruited to walk on a treadmill at different speeds and one subject was asked to perform free-walking on ground floor for three different walking speeds. Moreover, our algorithm was compared with two alternative methods from the literature. Comparison results confirmed the advantages of our method in adapting and accurately estimating the gait phase, especially when the walking speed is changing.

Our results showed that the advantages of our algorithm are threefold. First of all, our algorithm could provide continuous and accurate online gait phase estimation. Secondly, the intrinsic adaptivity of AOs guaranteed fast response to gait pattern variations without losing synchronization. Finally, the proposed algorithm also showed high performance in estimating the gait phase during free walking in an ecological walking scenario.

In future works, we expect to implement and validate a phase-dependent assistive strategy for lower-limb orthoses. The gait phase estimator could provide a reference for generating a control policy based on the superimposition of motor primitives. The feasibility and efficiency of this control policy would be evaluated through its effectiveness in reducing the efforts required for a locomotion task, for instance, by monitoring lower-limb muscle activation, or metabolic consumption through direct or indirect calorimeters.

Acknowledgements This work was supported by the EU within the CYBERLEGs project (FP7-ICT-2011-2.1 Grant Agreement #287894), by Fondazione Pisa within the IUVO project (prog. 154/11).

References

Ambrozic, L., Gorsic, M., Geeroms, J., Flynn, L., Molino Lova, R., Kamnik, R., et al. (2014). CYBERLEGs: A user-oriented robotic transfemoral prosthesis with whole-body awareness control. *IEEE Robotics and Automation Magazine*, *21*(4), 82–93.

Bollens, B., Crevecoeur, F., Detrembleur, C., Warlop, T., & Lejeune, T. M. (2014). Variability of human gait: Effect of backward walking and dual-tasking on the presence of long-range autocorrelations. *Annals of Biomedical Engineering*, *42*(4), 742–750.

Buchli, J., Righetti, L., & Ijspeert, A. J. (2008). Frequency analysis with coupled nonlinear oscillators. *Physica D: Nonlinear Phenomena*, *237*, 1705–1718.

Cappellini, G., & Ivanenko, Y. (2006). Motor patterns in human walking and running. *Journal of*, 3426–3437.

Crea, S., Donati, M., De Rossi, S. M. M., Oddo, C. M., & Vitiello, N. (2014). A wireless flexible sensorized insole for gait analysis. *Sensors (Basel, Switzerland)*, *14*(1), 1073–1093.

Donati, M., Vitiello, N., De Rossi, S. M. M., Lenzi, T., Crea, S., Persichetti, A., et al. (2013). A flexible sensor technology for the distributed measurement of interaction pressure. *Sensors (Basel, Switzerland)*, *13*(1), 1021–1045.

Giovacchini, F., Vannetti, F., Fantozzi, M., Cempini, M., Cortese, M., Parri, A., et al. (2014). A light-weight active orthosis for hip movement assistance. *Robotics and Autonomous Systems, 73, 123-134*.

Holgate, M. a, Sugar, T. G., & Alexander, W. B. (2009). A Novel Control Algorithm for Wearable Robotics using Phase Plane Invariants. In *IEEE International Conference on Robotics and Automation,* 3845–3850.

Iezzoni, L. I., McCarthy, E. P., Davis, R. B., & Siebens, H. (2001). Mobility difficulties are not only a problem of old age. *Journal of General Internal Medicine*, *16*, 235–243.

Iwasaki, T. (2008). Multivariable harmonic balance for central pattern generators. *Automatica*, *44*(12), 3061–3069.

Kao, P. C., Lewis, C. L., & Ferris, D. P. (2010). Invariant ankle moment patterns when walking with and without a robotic ankle exoskeleton. *Journal of biomechanics*, *43*(2), 203–209.

Kawamoto, H., Taal, S., Niniss, H., Hayashi, T., Kamibayashi, K., Eguchi, K., & Sankai, Y. (2010). Voluntary motion support control of Robot Suit HAL triggered by bioelectrical signal for hemiplegia. In *IEEE Engineering in Medicine and Biology Society. Conference*, 462–466.

Kazerooni, H., Steger, R., & Huang, L. (2006). Hybrid Control of the Berkeley Lower Extremity Exoskeleton (BLEEX). *The International Journal of Robotics Research*, *25*(5-6), 561–573.

Lenzi, T., Carrozza, M. C., & Agrawal, S. K. (2013). Powered hip exoskeletons can reduce the user's hip and ankle muscle activations during walking. *IEEE Transactions on Neural Systems and Rehabilitation Engineering*, *21*(6), 938–948.

Lewis, C. L., & Ferris, D. P. (2011). Invariant hip moment pattern while walking with a robotic hip exoskeleton. *Journal of biomechanics*, *44*(5), 789–793.

Pons, J. L. (2008). *Wearable robots: biomechatronic exoskeletons.* (J. L. Pons, Ed.). John Wiley and Sons.

Pratt, G. a., & Williamson, M. M. (1995). Series elastic actuators. In *Proceedings 1995 IEEE/RSJ International Conference on Intelligent Robots and Systems. Human Robot Interaction and Cooperative Robots,* 399–406.

Righetti, L., Buchli, J., & Ijspeert, A. J. (2006). Dynamic Hebbian learning in adaptive frequency oscillators. *Physica D: Nonlinear Phenomena*, *216*(2), 269–281.

Righetti, L., Buchli, J., & Ijspeert, A. J. (2009). Adaptive Frequency Oscillators and Applications. *The Open Cybernetics & Systemics Journal*, *3*(2), 64–69.

Ronsse, R., De Rossi, S. M. M., Vitiello, N., Lenzi, T., Carrozza, M. C., & Ijspeert, A. J. (2013). Real-Time Estimate of Velocity and Acceleration of Quasi-Periodic Signals Using Adaptive Oscillators. *IEEE Transactions on Robotics*, *29*(3), 783–791.

Ronsse, R., Lenzi, T., Vitiello, N., Koopman, B., Van Asseldonk, E., De Rossi, S. M. M., et al. (2011). Oscillator-based assistance of cyclical movements: Model-based and model-free approaches. *Medical and Biological Engineering and Computing*, *49*, 1173–1185.

Veneman, J. F., Ekkelenkamp, R., Kruidhof, R., van der Helm, F. C. ., & van der Kooij, H. (2006). A Series Elastic- and Bowden-Cable-Based Actuation System for Use as Torque Actuator in Exoskeleton-Type Robots. *The International Journal of Robotics Research*, *25*(3), 261–281.

Verghese, J., LeValley, A., Hall, C. B., Katz, M. J., Ambrose, A. F., & Lipton, R. B. (2006). Epidemiology of gait disorders in community-residing older adults. *Journal of the American Geriatrics Society*, *54*(2), 255–261.

Winter, D. a. (2009). *Biomechanics and motor control of human movement*. John Wiley and Sons.

Yan, T., Cempini, M., Oddo, C. M., & Vitiello, N. (2015). Review of assistive strategies in powered lower-limb orthoses and exoskeletons. *Robotics and Autonomous Systems*, *64*, 120–136.